Electronic Supplementary Material (ESI) for Journal of Materials Chemistry A.

Supporting Information

Hierarchical NiFeP microflowers direct grown on Ni foam for efficient electrocatalytic oxygen evolution

Jiahao Yu,[a] Gongzhen Cheng[a] and Wei Luo[a,b*]

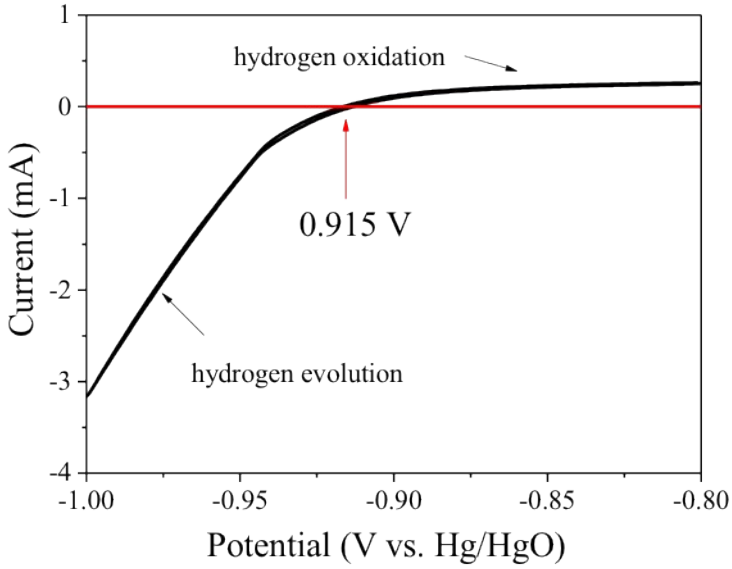

Figure S1. Potential calibration of the reference electrode in 1 M KOH solution. The average of the two potentials at which the current crossed zero was chosen to be the thermodynamic potential for the hydrogen electrode reaction. In 1 M KOH solution, $E_{RHE} = E_{Hg/HgO} + 0.915$ V.

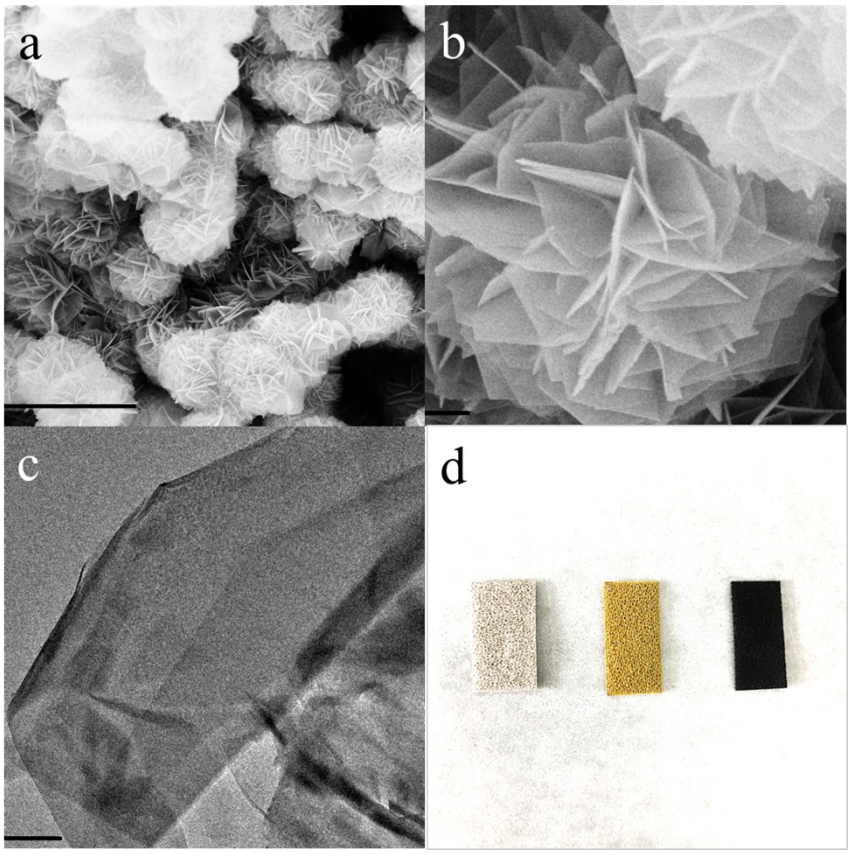

Figure S2. (a, b) SEM images and (c) TEM image of NiFe LDH. (d) Optical images of Ni foam, NiFe LDH and $(Ni_{0.5}Fe_{0.5})_2P$. Scale bars: (a)10 μm; (b) 500 nm; (c) 250 nm.

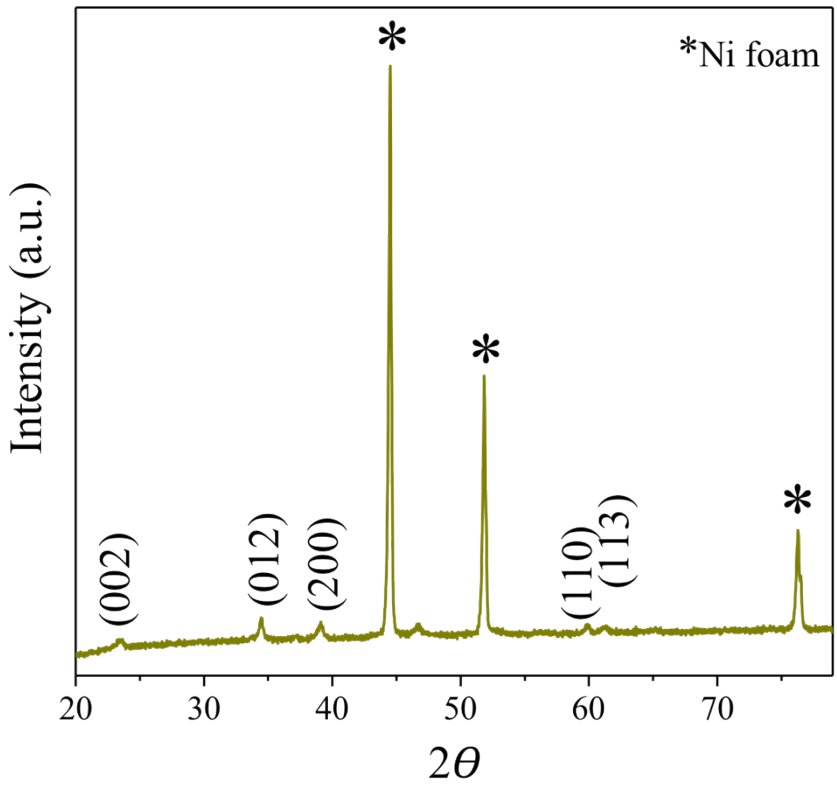

Figure S3. XRD pattern for NiFe LDH.

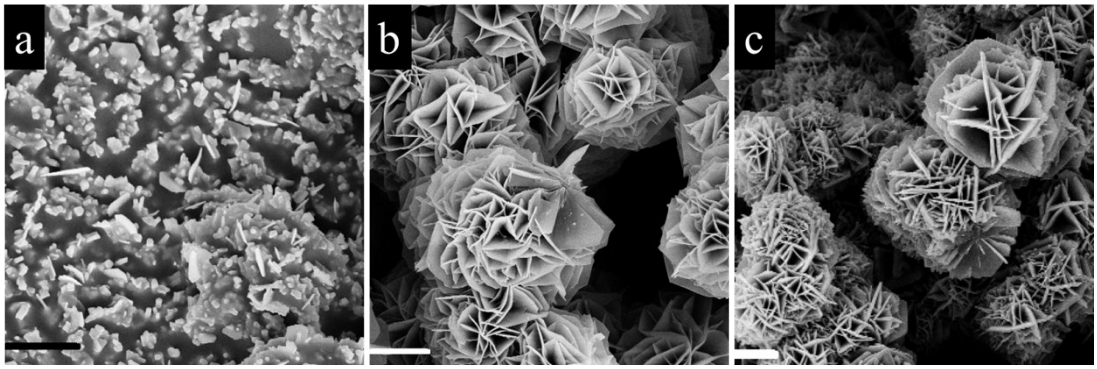

Figure S4. SEM images of (a) Ni_2P, (b) $(Ni_{0.75}Fe_{0.25})_2P$ and (c) $(Ni_{0.25}Fe_{0.75})_2P$. Scale bar: 2 μm.

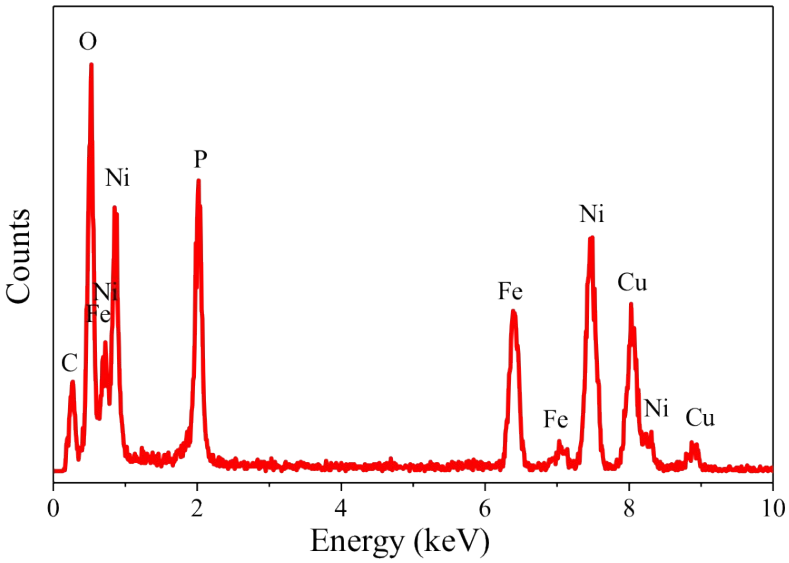

Figure S5. EDX spectrum of $(Ni_{0.5}Fe_{0.5})_2P$.

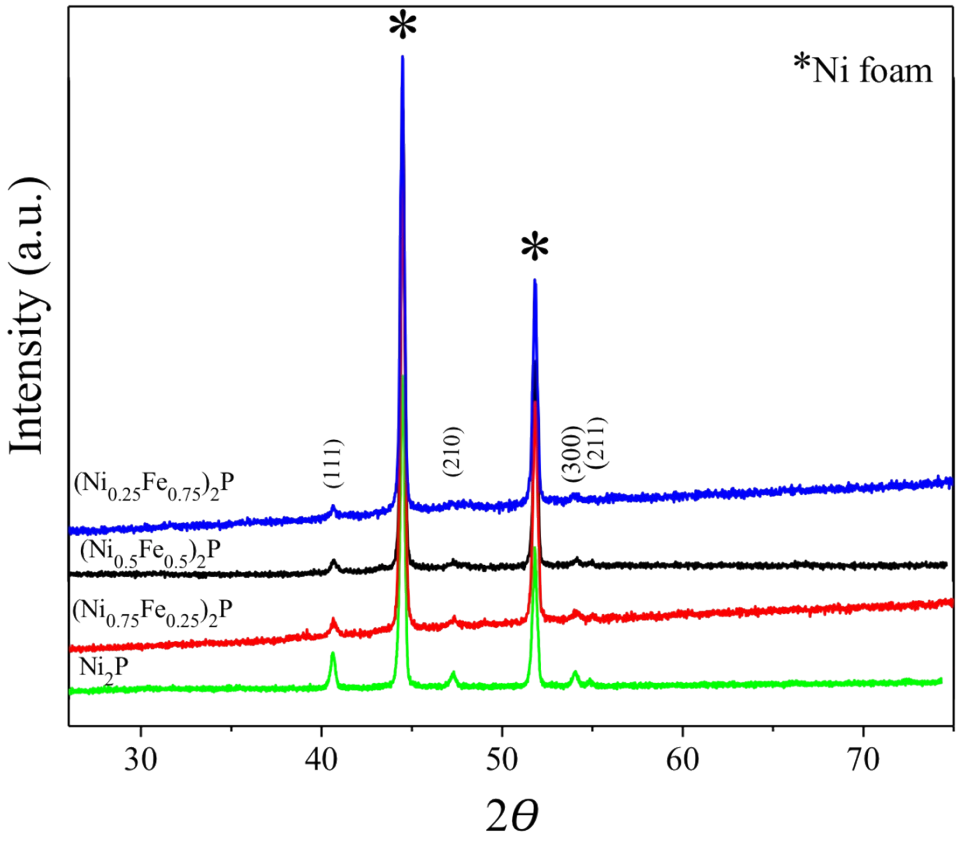

Figure S6. XRD pattern for $(Ni_xFe_{1-x})_2P$ (x=0.25, 0.5, 0.75) and Ni_2P.

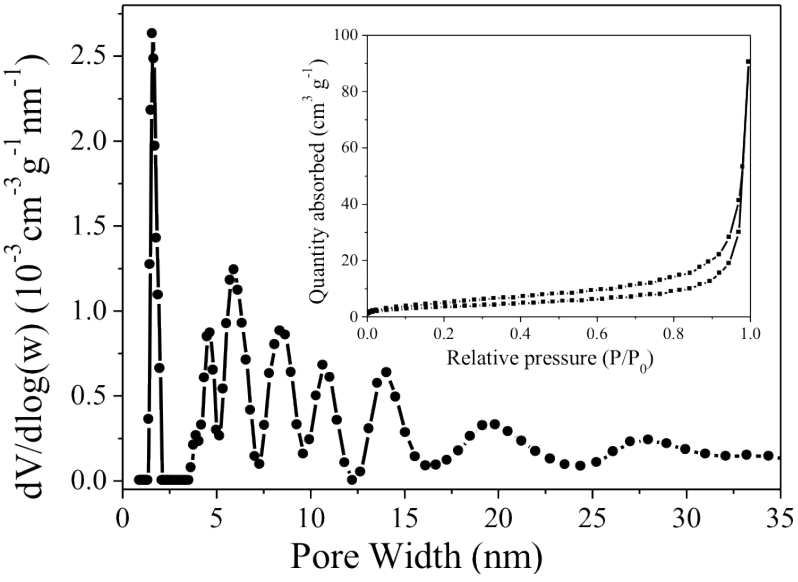

Figure S7. Pore size distribution (DFT model) of $(Ni_{0.5}Fe_{0.5})_2P$. Inset shows the N_2 adsorption-desorption isotherm.

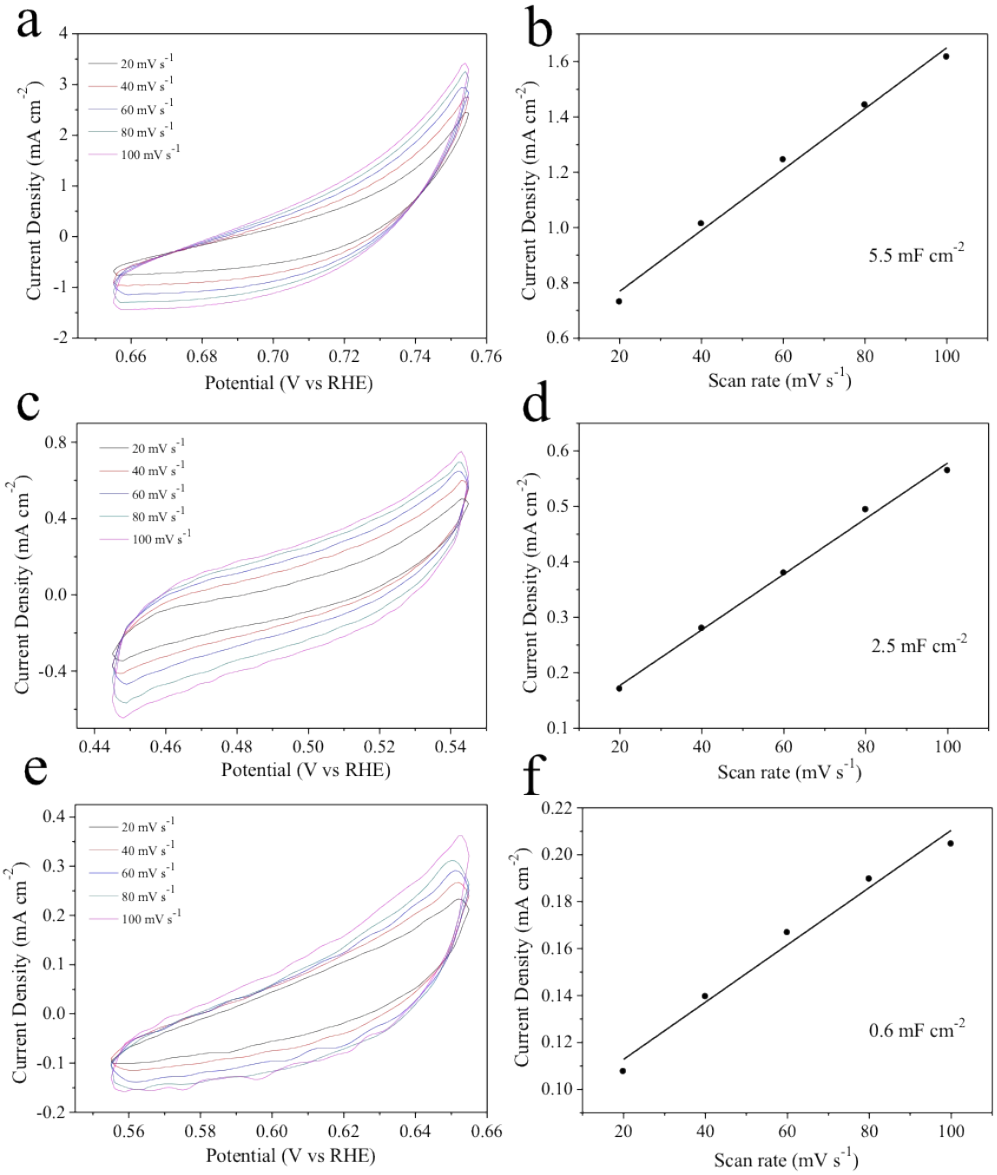

Figure S8. Cyclic voltammetry (CV) curves of (a) $(Ni_{0.5}Fe_{0.5})_2P$, (c) Ni_2P and (e) NiFe LDH tested at various scan rates from 20 to 100 mV s^{-1}. Scan rate dependence of the current densities of (b) $(Ni_{0.5}Fe_{0.5})_2P$, (d) Ni_2P and (f) NiFe LDH at 0.705 V, 0.495 V, 0.605 V (vs RHE), respectively.

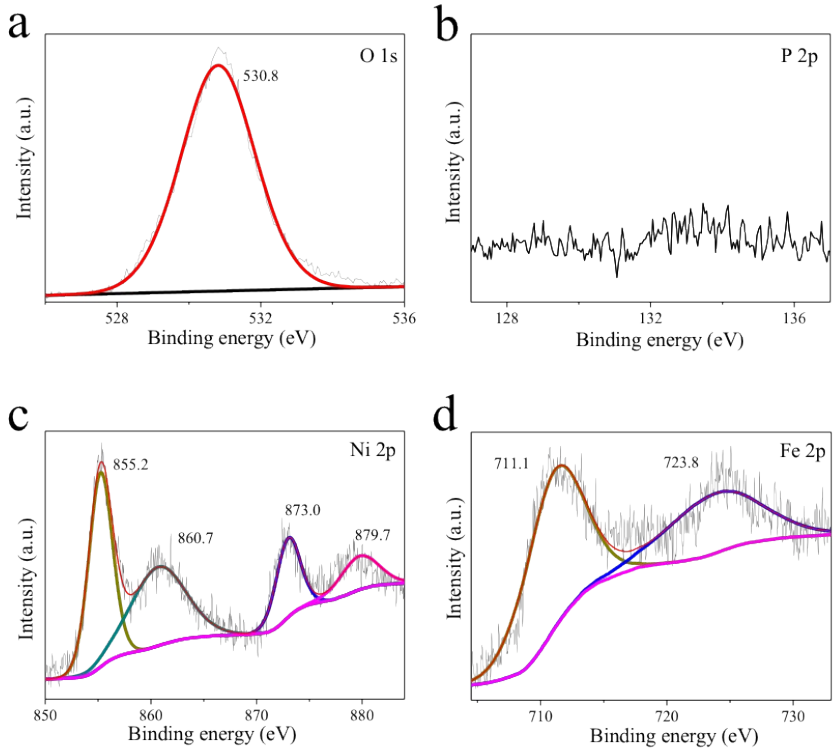

Figure S9. XPS spectra of $(Ni_{0.5}Fe_{0.5})_2P$ after OER.

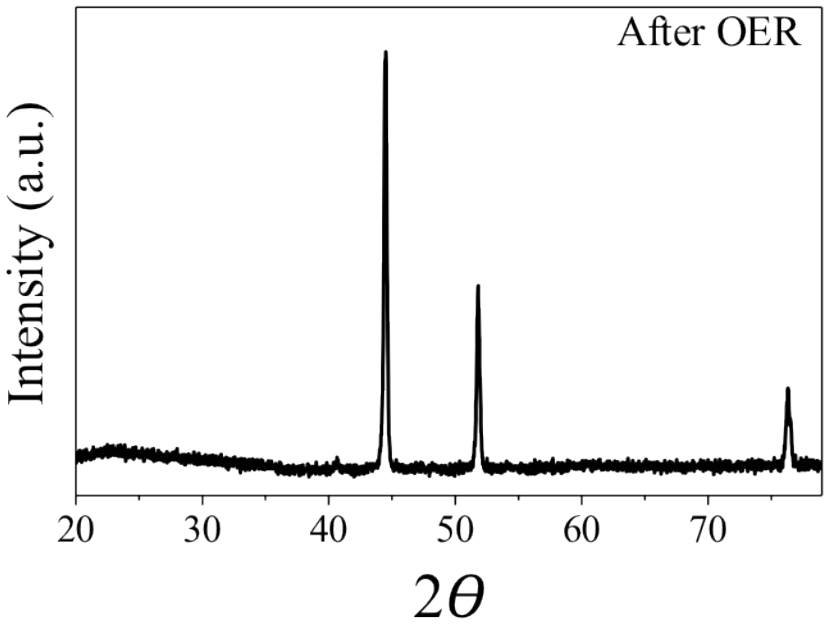

Figure S10. XRD pattern for $(Ni_{0.5}Fe_{0.5})_2P$ after long-term cycling.

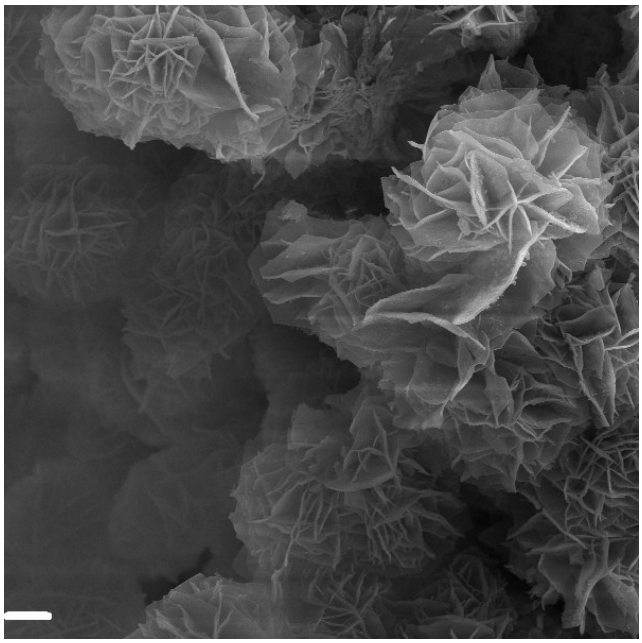

Figure S11. SEM image of $(Ni_{0.5}Fe_{0.5})_2P$ after long-term cycling. Scale bar: 2 μm.

Table S1 The actual atomic ratios of Ni, Fe and P of $(Ni_xFe_{1-x})_2P$ determined by ICP-AES.

$(Ni_xFe_{1-x})_2P$	**Ni (Atomic%)**	**Fe (Atomic%)**	**P (Atomic%)**
x=0.25	27.9	27.2	44.9
x=0.5	38.9	22.2	38.9
x=0.75	54.7	11.6	33.7

Table S2 Comparison of catalytic performance with other phosphides and NiFe based catalysts.

Materials	Current Density	Overpotential	Mass Loading	Reference
$(Ni_{0.5}Fe_{0.5})_2P$	10 mA cm^{-2}	203 mV	3 mg cm^{-2}	This work
	20 mA cm^{-2}	219 mV		
	30 mA cm^{-2}	231 mV		
	50 mA cm^{-2}	251 mV		
NiFeP	10 mA cm^{-2}	277 mV	---	[1]
$(Ni_{0.51}Co_{0.49})_2P$	10 mA cm^{-2}	239 mV	---	[2]
NiCoP	50 mA cm^{-2}	308 mV	5 mg cm^{-2}	[3]
Ni/NiP	30 mA cm^{-2}	270 mV	11 mg cm^{-2}	[4]
$NiOOH/Ni_5P_4$	10 mA cm^{-2}	290 mV	3.5 mg cm^{-2}	[5]
Co-P	30 mA cm^{-2}	330 mV	0.1 mg cm^{-2}	[6]
CoMnP	10 mA cm^{-2}	330 mV	0.28 mg cm^{-2}	[7]
FeP-rGO@CFP	10 mA cm^{-2}	260 mV	---	[8]
Ni_2P	10 mA cm^{-2}	290 mV	0.14 mg cm^{-2}	[9]
Sandwiched NiFe/C arrays	20 mA cm^{-2}	220 mV	1.3 mg cm^{-2}	[10]
NiFe LDH	10 mA cm^{-2}	224 mV	1 mg cm^{-2}	[11]
NiFe/RGO	10 mA cm^{-2}	245 mV	1 mg cm^{-2}	[12]
NiFeMo	10 mA cm^{-2}	280 mV	0.28 mg	[13]

			cm^{-2}	
FeNi-O	10 mA cm^{-2}	213 mV	0.254 mg cm^{-2}	[14]
NiFe LDH	10 mA cm^{-2}	240 mV	---	[15]
$FeNi_8Co_2$ LDH	10 mA cm^{-2}	220 mV	0.25 mg cm^{-2}	[16]
$Ni_{2/3}Fe_{1/3}$-rGO	10 mA cm^{-2}	230 mV	0.25 mg cm^{-2}	[17]
NiFe-NS	10 mA cm^{-2}	300 mV	1 mg cm^{-2}	[18]

References

1 C. G. Read, J. F. Callejas, C. F. Holder, R. E. Schaak, *Appl. Mater. Interfaces,* 2016, **8**, 12798.

2 J. Yu, Q. Li, Y. Li, C.-Y. Xu, V. P. Dravid, *Adv. Funct. Mater.,* 2016, **26**, 7644.

3 Y. Li, H. Zhang, M. Jiang, Y. Kuang, X. Sun, X Duan, *Nano Res,* 2016, **9**, 2251.

4 G.-F. Chen, T. Y. Ma, Z.-Q. Liu, N. Li, Y.-Z. Su, K. Davey, S. Z. Qiao, *Adv. Funct. Mater*., 2016, **26**, 3314.

5 M. Ledendecker, S. K. Calderón, C. Papp, H.-P. Steinrück, M. Antonietti, M. Shalom, *Angew. Chem. Int. Ed*., 2015, **54**, 12361.

6 Y. Yang, H. Fei, G. Ruan, J. M. Tour, *Adv. Mater.,* 2015, **27**, 3175.

7 D. Li, H. Baydoun, C. N. Verani, S. L. Brock, *J. Am. Chem. Soc.,* 2016, **138**, 4006.

8 J. Masud, S. Umapathi, N. Ashokaan, M. Nath, *J. Mater. Chem. A*, 2016, **4**, 9750.

9 L.-A. Stern, L. Feng, F. Song, X. Hu, *Energy Environ. Sci*., 2015, **8**, 2347.

10 Y. Feng, H. Zhang, L. Fang, Y. Mu, Y. Wang, *ACS Catal*., 2016, **6**, 4477.

11 Z. Li, M. Shao, H. An, Z. Wang, S. Xu, M. Wei, D. G. Evans, X. Duan, *Chem. Sci.,* 2015, **6**, 6624.

12 D. H. Youn, Y. B. Park, J. Y. Kim, G. Magesh, Y. J. Jang, J. S. Lee, *Journal of Power Sources,* 2015, **294**, 437.

13 N. Han, F. Zhao, Y. Li, *J. Mater. Chem. A,* 2015, **3**, 16348.

14 X. Long, Z. Ma, H. Yu, X. Gao, X. Chen, S. Yang, Z. Yi, *J. Mater. Chem. A,* 2016, **4**, 14939.

15 J. Luo, J.-H. Im, M. T. Mayer, M. Schreier, M. K. Nazzeeruddin, N.-G. Park, S. D. Tilley, H. J. Fan, M. Grätzel, *Science*, 2014, **345**, 1593.

16 X. Long, S. Xiao, Z. Wang, X. Zheng, S. Yang, Chem. Commun., 2015, **51**, 1120.

17 W. Ma, R. Ma, C. Wang, J. Liang, X. Liu, K. Zhou, T. Sasaki, *ACS Nano*., 2015, **9**, 1977.

18 F. Song, X. Hu, *Nat. Commun*., 2014, **5**, 4477.